Updating Land Use Land Cover City of Baubau

Rini Anggraini [1*], Sumbangan Baja[1], and Risma Neswati[1]
[1]Department of Soil Science, Faculty of Agricultural Sciences, Hasanuddin University, Indonesia
*agrrrini@gmail.com

Abstract *Land use and land cover (LULC) mapping is a crucial instrument in spatial planning and environmental management, particularly in urban areas with high spatial dynamics. This study aims to update the LULC map of BauBau City (study area 28,619 ha) using Landsat 8 imagery (September 2024). The method employed is supervised classification using the Maximum Likelihood Classification (MLC) algorithm, supplemented by manual interpretation to enhance classification accuracy. The research process includes data pre-processing (geometric, radiometric, and atmospheric corrections), image classification, and accuracy testing using the Stratified Random Sampling approach at 300 reference points. The initial classification results identified five land cover classes, which were then refined through manual interpretation to produce five main classes: forest, agriculture, built-up land, open land, and water bodies. The evaluation yielded an overall accuracy of 91.7% and a Kappa coefficient of 0.843, indicating an extreme level of classification suitability for field conditions. This combined approach has proven effective in enhancing the spatial and thematic representation of LULC mapping and can support sustainable, data-driven urban development planning.*

Keywords: LULC, Landsat 8, MLC classification, manual interpretation, spatial accuracy

Introduction

Land use and land cover (LULC) mapping is a key approach to understanding the spatial dynamics of a region, particularly in urban areas (Hersperger et al., 2018; Lu et al., 2022; H. Wu et al., 2021). First developed in the early 1970s using aerial photography and analog imagery (Loveland, 2012), this technique has evolved with advances in remote sensing and Geographic Information Systems (GIS) technology. GIS integration enhances the ability to analyze spatially and visualize dynamic and continuous changes in LULC (Yin et al., 2021).

Satellite sensors such as the Landsat Multispectral Scanner (MSS), Thematic Mapper (TM), and Enhanced Thematic Mapper Plus (ETM+) have enabled more accurate regional-scale LULC mapping (Gómez et al., 2016; Masek et al., 2001). In the past decade, the arrival of Landsat 8 and Sentinel-2 has provided significant improvements in spatial, spectral, and temporal resolution, thus greatly supporting periodic and more detailed monitoring of LULC changes (Shen et al., 2022, 2023; Tran et al., 2022; J. Wu et al., 2022). Landsat 8, with its Operational Land Imager (OLI) and Thermal Infrared Sensor (TIRS) sensors providing 11 spectral channels, is widely used for mapping urban and tropical areas due to its ability to accurately detect land cover variations (Roy et al., 2014). Several studies have

shown that the Landsat 8 spectral configuration is effective in supporting spatial and thematic analysis, including in the context of land-use planning and resource management in tropical regions such as Indonesia (Baja et al., 2007; Baja et al., 2019a; Hakim et al., 2021). Spatial use conflicts and uncontrolled land-use changes have also been studied in South Sulawesi by Baja et al. (2019b), who emphasized the importance of regular LULC data updates for cities like BauBau.

In an urban context, changes in LULC are closely related to urbanization processes, which impact green open spaces (Negesse et al., 2024), surface water flow (Shrestha et al., 2021), air quality (Islam et al., 2024; Li et al., 2019), and ambient temperature (Halefom et al., 2024). In BauBau City, population growth and development activities over the past five years (2018–2023) indicate significant changes in land use patterns, although comprehensive historical data is still limited (Aldiansyah & Risna, 2024). Therefore, updating LULC data is crucial to support spatial planning, environmental management, and urban risk mitigation.

In various land use and land cover mapping studies, selecting the right classification method is crucial, especially for complex urban areas. Previous studies have shown that supervised approaches supplemented with visual validation, such as manual interpretation, tend to produce more accurate results than fully automated methods (Lunetta et al., 2006; Roy et al., 2014). Therefore, a combined approach is often employed to enhance both thematic and spatial accuracy in LULC mapping.

This article focuses on updating the LULC map of BauBau City using Landsat 8 imagery, using a supervised approach (MLC) combined with manual interpretation. The goal is to produce an accurate and up-to-date LULC map to support sustainable urban planning based on spatial data.

Research Location

BauBau City is located in the south of Buton Island, Southeast Sulawesi, with an area of 295.07 km². Its varied geographic characteristics, spanning coastal areas, lowlands, and hills, make this region quite complex in terms of land use and cover. This is consistent with the findings of Baja et al. (2012), who emphasized that coastal and hilly areas in Sulawesi require different spatial approaches in land use planning. The city was chosen as the research location due to its

role as a center of economic activity and interregional connectivity in the Buton Islands. Rapid population growth and infrastructure development in recent years have driven significant land use changes (Suarmawati, 2023). Therefore, updated information on land use and cover in BauBau is needed to support more responsive and sustainable spatial planning.

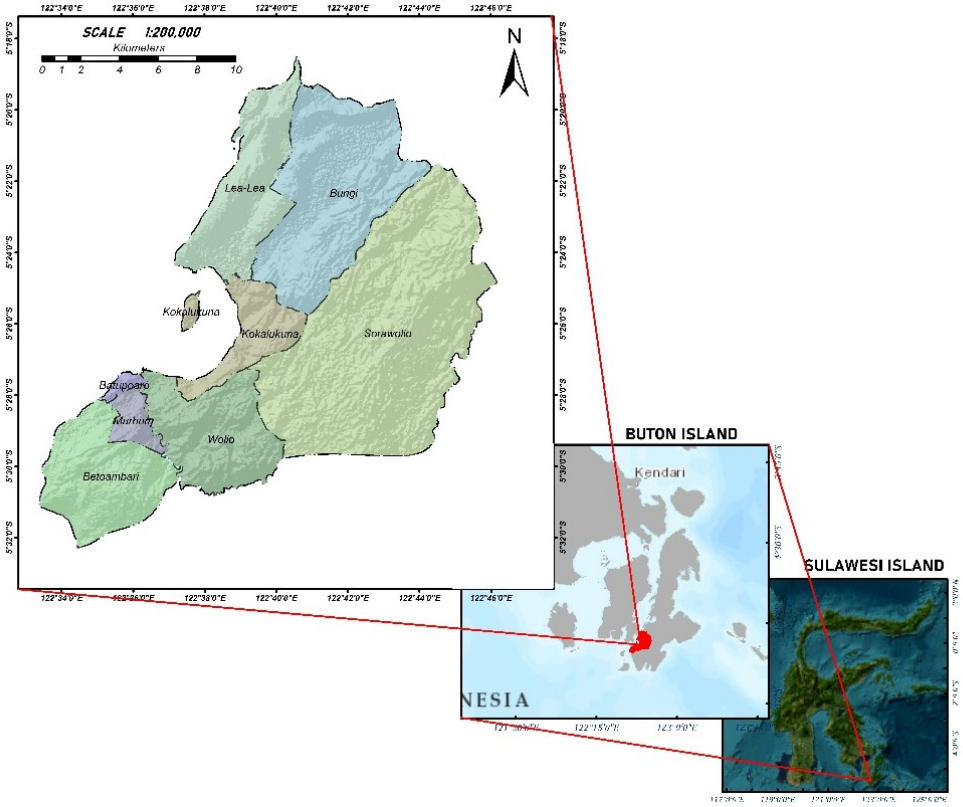

Figure 1. Research Location Map

Data

This study used Landsat 8 imagery from 2024 (September 2024) with <5% cloud cover in the study area as the primary data, with a spatial resolution of 30 meters and appropriate temporal coverage. Landsat 8 is equipped with OLI and TIRS, which together provide a total of 11 spectral bands: nine optical bands, one panchromatic band, and two thermal bands (all resampled to 30 m). This spectral and spatial configuration is very supportive for the analysis of land use and land cover changes in tropical areas such as BauBau City (Roy et al., 2014; USGS, 2019).

Administrative boundary maps are used as supporting data to facilitate regional identification and validate spatial analysis results. Administrative boundary maps are obtained in shapefile format (EPSG:4326) from the official Inageoportal portal (2024).

Research Methods

This study utilizes a combined approach between Geographic Information Systems (GIS) and Remote Sensing to analyze land use and cover (LULC) in BauBau City in 2024. In the LULC study, image classification methods include unsupervised techniques such as the K-Means and ISODATA algorithms (Paradis, 2022; Ruggeri et al., 2021; Singh & Singh, 2018), and supervised techniques that require training data, such as Maximum Likelihood Classification (MLC) and Support Vector Machine (SVM) (M. S. Chowdhury, 2024; S. Chowdhury, 2024; Noer & Wibowo, 2024). Object-based approaches (OBIA), combining image segmentation and feature classification, have also been widely used (Blaschke, 2010; Kucharczyk et al., 2020). In addition, a fuzzy logic model for defining spatially based land management units has been developed by Baja et. Al (2002), which is relevant for improving thematic accuracy in heterogeneous areas.

This study used a combination of supervised classification with the Maximum Likelihood Classification (MLC) algorithm in ArcGIS 10.8 and manual interpretation by examining Google Earth Pro imagery. This approach was chosen to improve the accuracy of the classification results, particularly in areas with high heterogeneity. Manual interpretation served as additional validation to correct the automatic classification results, particularly for unclear or overlapping class boundaries, and to add LULC classes that could not be identified properly automatically.

Methodology

Figure 2 shows the research flow: image data pre-processing stage, image classification (supervised MLC algorithm method and manual interpretation), and accuracy testing to ensure that the resulting LULC map is accurate and represents actual conditions in BauBau City.

Data Pre-Processing

Satellite image preprocessing is a crucial step aimed at improving the visual quality, spatial consistency, and radiometric accuracy of data before entering the land use and cover classification process (Chander et al., 2009; Roy et al., 2014). This study used 2024 Landsat 8 imagery obtained through the USGS Earth Explorer and Copernicus Open Access Hub platforms (Radeloff et al., 2022; Wulder et al., 2022). The series of preprocessing steps applied included geometric correction, radiometric correction, band composite creation, atmospheric correction, and image cropping according to administrative boundaries.

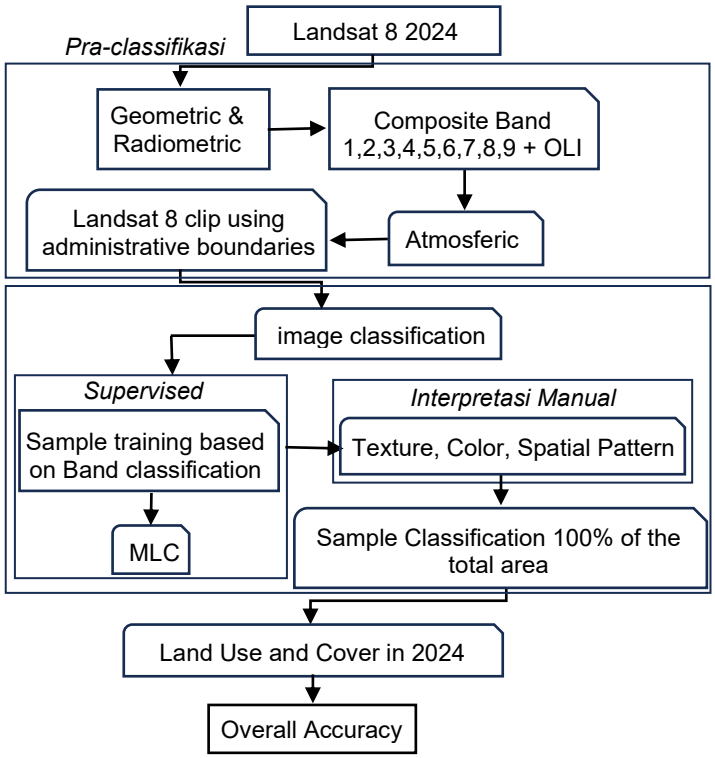

Figure 2. Research flowchart

The initial stage is geometric correction to eliminate spatial distortion due to topography, although the Level-1 Terrain Corrected (L1T) image has been orthorectified with DEM and GCP (USGS, 2019). Next, the image is projected to UTM zone 51S (WGS 1984 datum) to match other vector data. To facilitate spectral differentiation between land classes (such as forest, settlement, water, or open land), radiometric correction is performed on each band using the empirical formula:

$$\rho TOA_{\lambda} = \frac{(0.0002\ X\ DN) - 0.1}{-0.90014722}$$

Calibration coefficients (rescaling factor Mλ = 0.00002; offset Aλ = −0.1) refer to USGS (2019). This calibration was calculated using the ENVI 5.5 platform before DOS correction was applied. To prepare for interpretation and classification, such as vegetation, water bodies, and built-up areas, band composites were created by combining Landsat 8 spectral channels (11 bands). Examples of combinations are: 5-4-3 (NIR, Red, Green) and 6-5-4 (SWIR, NIR, Red) to clarify visual features (Biney et al., 2022). Atmospheric correction using the Dark Object Subtraction (DOS) method was applied to reduce atmospheric effects and improve classification accuracy (Chavez, 1988). The final pre-processing stage was image clipping

according to the administrative boundaries of BauBau City, so that the analysis only covers the study area.

Data Processing

Supervised Classification

Supervised image classification begins with the selection of training samples based on visual interpretation of Landsat 8 imagery and a combination of composite bands to distinguish each class. The water class uses bands 5-6-4 because water appears dark in NIR (band 5). Settlements use bands 7-6-4 to highlight artificial materials, and vegetation uses bands 6-5-2, which are sensitive to chlorophyll.

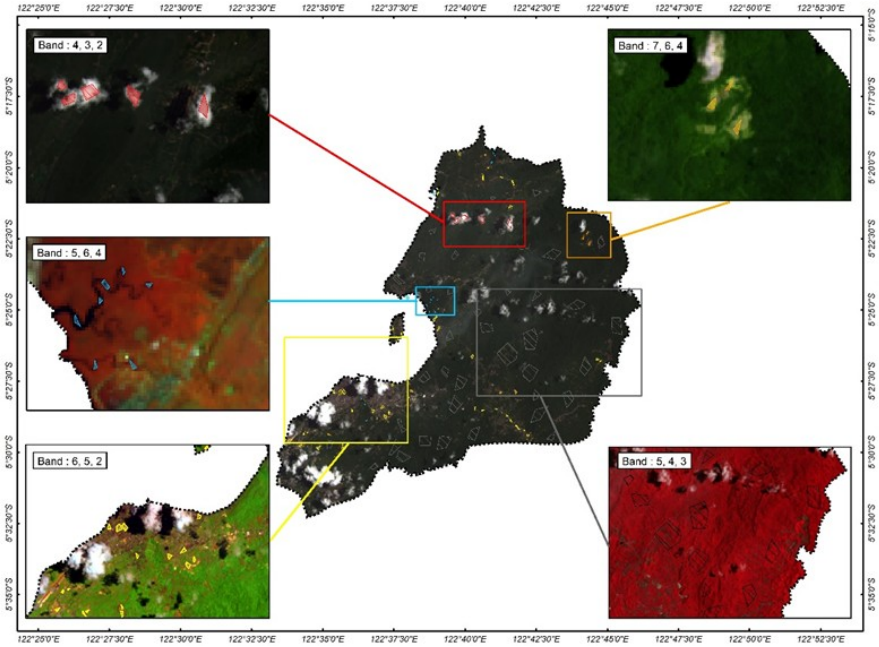

Figure 3. Band classification process map

After collecting training samples, classification is performed using the Maximum Likelihood Classification (MLC) algorithm, which determines the class of each pixel based on the highest probability of the training sample's statistical value. The result is a land use and land cover map showing the spatial distribution of each class, depending on the quality of the samples used.

Manual Interpretation

After initial classification using supervised methods, manual interpretation is performed to refine the results and increase spatial and thematic accuracy. This stage begins with converting the classification results from raster to vector (polygon) to correct areas of misclassification.

Manual interpretation is performed by comparing the classification results with reference data such as high-resolution imagery, thematic maps, or field data to correct misclassifications. This process involves three stages: (1) cloud masking to remove cloud-covered areas, (2) classification correction to correct incorrect class labels, and (3) land reclassification to adjust thematic classes based on visual interpretation.

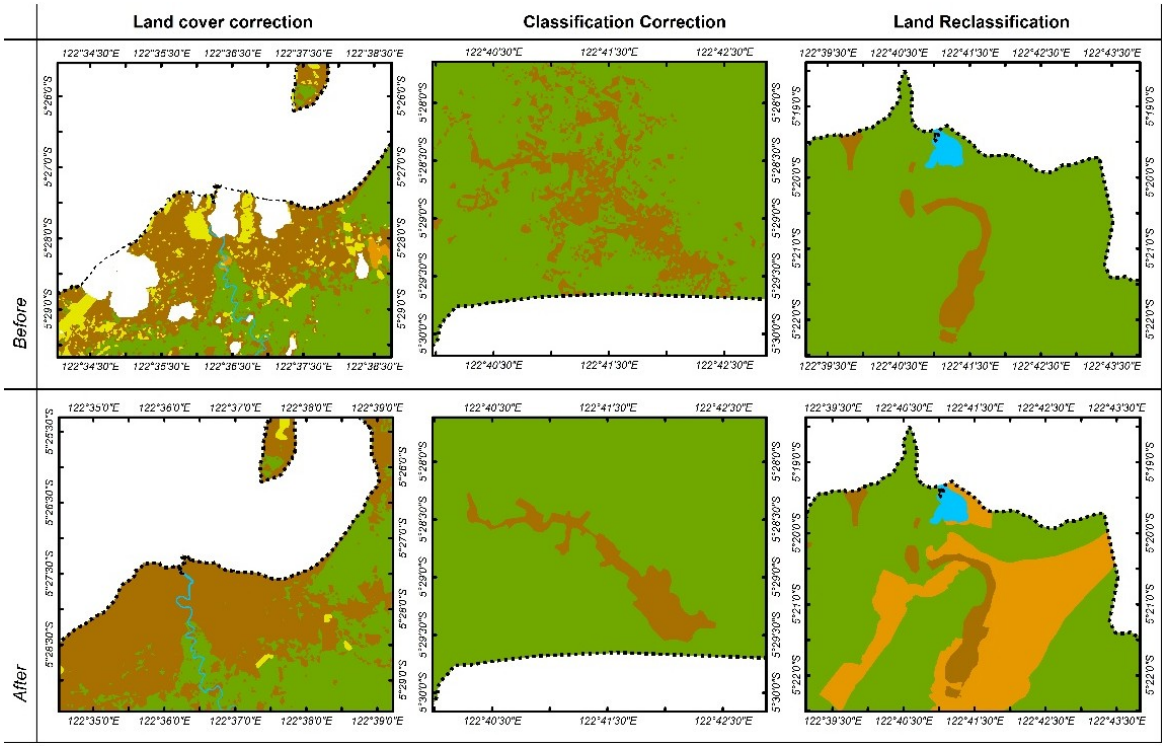

Figure 4. Supervised misclassification correction

All these stages are part of post-classification refinement, which aims to increase the reliability of classification results visually, spatially, and thematically, so that they are more accurate and reflect field conditions.

Accuracy test

Accuracy testing was conducted to assess the suitability of the 2024 land use and land cover classification results to field conditions using the Stratified Random Sampling method. A total of 300 sample points were taken proportionally to the area of each class using the Create Accuracy Assessment Points tool in ArcGIS. These points were validated against reference data, and the Overall Accuracy (OA) was calculated as an indicator of classification accuracy and reliability of the 2024 LULC map.

Results and Discussion

This section presents the main results of the 2024 BauBau City LULC image classification process. The process included supervised classification, manual interpretation for visual correction, and accuracy testing to assess the reliability of the results. The final results are maps and area distributions for each class that reflect actual conditions in the field.

Supervised Classification

Supervised classification (MLC) identified five LULC classes in BauBau City, with a total classified area of 28,619.11 ha. The distribution of each class is listed in Table 1.

Table 1. Supervised classification result class.

Region	Name	Area (ha)
BauBau City	Forest	21590.05
	Built-up Land	4101.22
	Waterbodies	527.60
	Bare Land	586.45
	Could	1813.78
Total		**28619.11**

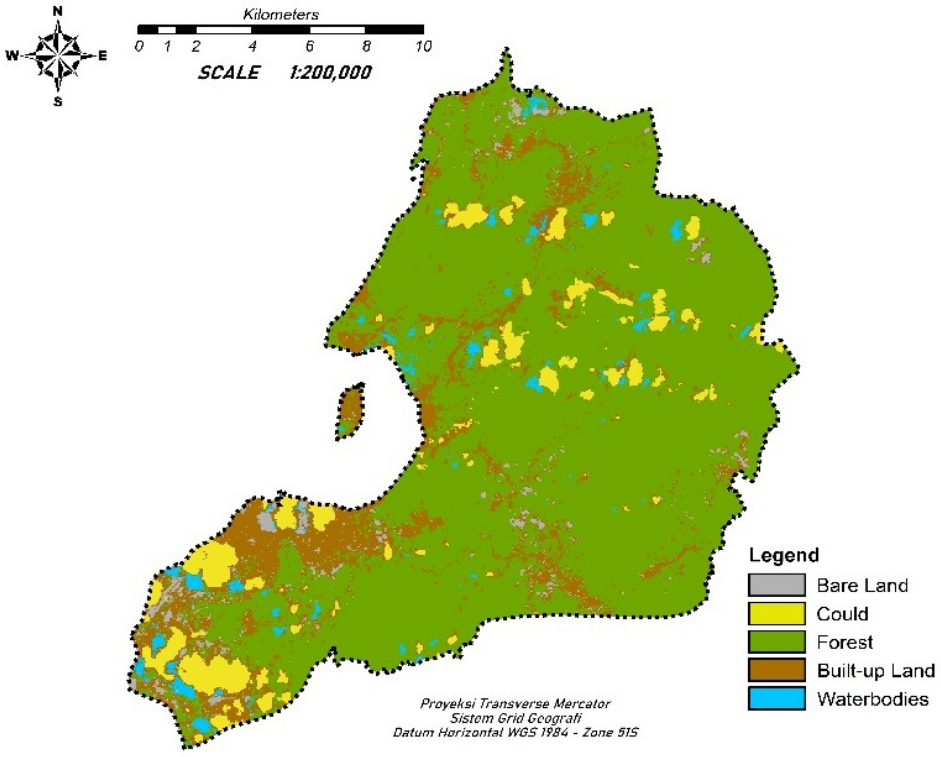

Figure 5. Land Use and Land Cover

The presence of cloud classes highlights the limitations of automated classification methods in handling atmospheric noise, which can lead to misclassification. While these methods are efficient and capable of processing large-scale data, their thematic accuracy remains limited, particularly in distinguishing classes with similar spectral characteristics and detecting small objects.

Manual Interpretation

Manual interpretation was applied post-supervised to detect new classes and correct errors using high-resolution imagery. This image-based adjustment resulted in land use and cover data that were more representative of actual conditions in the field, including the agricultural class (5,539.35 ha) that was previously undefined in the supervised results. Forest area was adjusted to 19,406.15 ha, built-up land was reduced to 3,179.36 ha, and the cloud class was eliminated. Although more time-consuming, this approach proved effective in producing more accurate and detailed classifications, especially in areas with high levels of complexity. The final interpretation results are presented in Table 2 and Figure 6.

Table 2. Classification results of manual interpretation

Region	Landcover	Area (ha)
BauBau City	Forest	19406.15
	Built-up Land	177.00
	Bare Land	3179.36
	Agriculture	5539.35
	Waterbodies	317.26
Total		**28619.11**

Accuracy assesment

This study tested the accuracy of the 2024 land use and cover image classification results using the Stratified Random Sampling method with 300 sample points distributed proportionally across each land cover class. The resulting classification labels were compared with reference labels based on visual interpretation of high-resolution imagery. Evaluation was carried out through the preparation of a confusion matrix and the calculation of accuracy metrics, namely Overall Accuracy (OA), Producer's Accuracy (PA), User's Accuracy (UA), and the Kappa coefficient (κ).

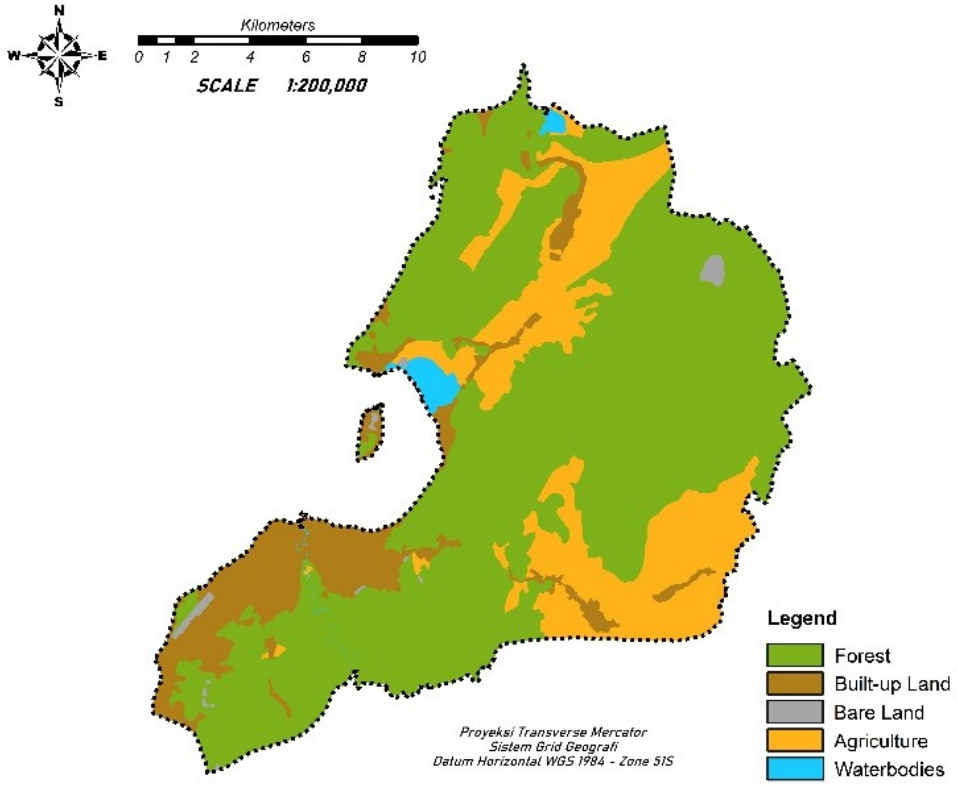

Figure 6. Manual interpretation classification map

Table 3. Accuracy test calculation value

Classification	Total Reference (r_i)	Total Prediction (c_i)	Correct (x_{ii})	PA (%)	UA (%)
Forest	188	203	174	100.0	92.6
Agriculture	54	58	54	100.0	93.1
Built-up Land	29	33	26	89.7	78.8
Bare Land	14	2	2	14.3	100.0
Waterbodies	7	4	4	57.1	100.0

The accuracy value is calculated using the following formula:

$$OA = \frac{\sum a_{ii}}{N} \; X \; 100\%$$

$$PA = \frac{a_{ii}}{Total\ column\ i} \; X \; 100\%$$

$$UA = \frac{a_{ii}}{Total\ row\ i} \; X \; 100\%$$

$$K = \frac{N \sum a_{ii} - \sum(R_i \cdot C_i)}{N - \sum(R_i \cdot C_i)} \; X \; 100\% = 0.843$$

Information:

a_{ii} : Number of correct classifications in class iv

R_i : Number of pixels resulting from classification in class I (row)

C_i : Number of references of class i (column)

N : Total sample points (300 points)

The analysis results showed an Overall Accuracy of 91.7%, indicating that most of the classification results were consistent with the reference data. The highest Producer's Accuracy (PA) was observed in the forest and agriculture classes, both reaching 100%, while the lowest PA was found in open land (14.3%) and water bodies (57.1%). The low PA value for open land is mainly due to the frequent presence of dry vegetation, which exhibits spectral characteristics similar to built-up areas, making it difficult for the Maximum Likelihood Classification (MLC) method to distinguish between these classes. In addition, narrow water bodies are often confused with thin cloud shadows in the NIR band, resulting in lower classification accuracy. The highest User's Accuracy (UA) was recorded for open land and water bodies (100%), whereas the built-up land class showed the lowest UA value (78.8%). PA values exceeding 100% may occur due to sampling bias or minor classification errors that cause overprediction in that class. From these calculations, the Kappa Coefficient value of 0.843 indicates a very strong level of agreement between the classification results and the reference, after correcting for random match probabilities. This spatial-based accuracy evaluation approach has been widely used in Indonesian LULC studies to improve the reliability of thematic maps in the context of regional planning (Hakim et al., 2021, 2022).

Discussion

The combined method of supervised classification and manual interpretation successfully improved thematic and spatial accuracy in land use and cover mapping. This aligns with previous studies showing that integrating spatial approaches and thematic interpretation results in more optimal land use decisions, particularly in areas with land use conflicts such as South Sulawesi (Baja et al., 2019b). Successful classification begins with image preprocessing stages (geometric, atmospheric, and mosaic correction), which play a crucial role in matching spectral values and spatial position. This evaluation reflects the application of spatial validation principles as described in the DSS approach by Baja et al. (2007), resulting in data ready for analysis.

The selection of the appropriate band composite affects the quality of the training sample, as bands with high spectral contrast between classes can improve classification accuracy. In the initial classification, the results showed the presence of a cloud class covering 1,813.78 ha, a forest area of 21,590.05 ha, and an agricultural class that had not been specifically detected due to spectral overlap. With manual interpretation based on high-resolution imagery and raster-to-vector conversion, thematic and spatial corrections were performed. The cloud class was eliminated, the forest area decreased to 19,406.15 ha, and the agricultural class was identified as covering 5,539.35 ha.

Supervised classification excels in efficiency and large data processing, but is limited in distinguishing spectrally similar objects. In contrast, manual interpretation is more visually precise but requires more time and resources. The combination of the two produces more accurate and representative maps, especially in complex areas, and supports more reliable spatial-based decision-making.

Conclusion

This study demonstrates that updating the 2024 BauBau City Land Cover Map (LULC) can be effectively implemented by combining supervised classification (MLC) and manual interpretation based on high-resolution imagery. The initial classification identified five main classes. Manual interpretation enhanced class detection and corrected errors, resulting in five land cover classes that are more representative of actual conditions. Accuracy evaluation using 300 validation points yielded an overall accuracy of 91.7% and a Kappa coefficient of 0.843, indicating extreme classification reliability.

This combined approach has been proven to improve thematic and spatial accuracy, particularly in highly complex urban areas. The resulting LULC maps can be used as a basis for decision-making in spatial planning, resource management, and environmental impact mitigation in BauBau City. Going forward, regular data updates and high-resolution data integration will support evidence-based, sustainable urban planning.

References

Aldiansyah, S., & Risna, (2024). Urban Heat Island Detection on Urban Development Using Remote Sensing in BauBau City. ResearchGate. https://www.researchgate.net/publication/381092077

Baja, S. (2007). Spatial-based compromise programming for multiple criteria decision making in land use planning. Environmental Modeling and Assessment, 12(3), 171–184. https://doi.org/10.1007/s10666-006-9059-1

Baja, S. (2012). Perencanaan Tata Guna Lahan dalam Pengembangan Wilayah: Pendekatan Spasial dan Aplikasinya. Penerbit Andi.

Baja, S., Chapman, D. M., & Dragovich, D. (2002). A conceptual model for defining and assessing land management units using a fuzzy modeling approach in a GIS environment. Environmental Management, 29(5), 647–661. https://doi.org/10.1007/s00267-001-0053-8

Baja, S., Neswati, R., & Arif, S. (2019a). Using Geospatial Information Technology for Regional Assessment of Food Crop Land in South Sulawesi. IOP Conference Series: Earth and Environmental Science, 279(1), 012009. https://doi.org/10.1088/1755-1315/279/1/012009

Baja, S., Pulubuhu, D. A. T., Neswati, R., Arif, S., & Nurmiaty. (2019b). Land Use Conflict with a Particular Reference to Spatial Planning Implementation in South Sulawesi. IOP Conference Series: Earth and Environmental Science, 279(1), 012006. https://doi.org/10.1088/1755-1315/279/1/012006

Biney, E., Biney, N., Dadzie, I., Harris, E., Quartey, G. A., Asare, Y. M., Bessah, E., & Forkuo, E. K. (2022). Impact of mining on vegetation cover: A case study of Prestea Huni-Valley municipality. Scientific African, 17, e01387. https://doi.org/10.1016/j.sciaf.2022.e01387

Chander, G., Markham, B. L., & Helder, D. L. (2009). Summary of current radiometric calibration coefficients for Landsat MSS, TM, ETM+, and EO-1 ALI sensors. Remote Sensing of Environment, 113(5), 893–903. https://doi.org/10.1016/j.rse.2009.01.007

Chavez, P. S. (1988). An improved dark-object subtraction technique for atmospheric scattering correction of multispectral data. Remote Sensing of Environment, 24(3), 459–479. https://doi.org/10.1016/0034-4257(88)90019-3

Gómez, C., White, J. C., & Wulder, M. A. (2016). Optical remotely sensed time series data for land cover classification: A review. ISPRS Journal of Photogrammetry and Remote Sensing, 116, 55–72. https://doi.org/10.1016/j.isprsjprs.2016.03.008

Hakim, A. M. Y., Baja, S., Rampisela, D. A., & Arif, S. (2021). Modeling land use/land cover changes prediction using multi-layer perceptron neural network (MLPNN): A case study in Makassar City, Indonesia. International Journal of Environmental Studies, 78(2), 301–318. https://doi.org/10.1080/00207233.2020.1804730

Hakim, A. M. Y., Baja, S., Rampisela, D. A., & Arif, S. (2022). Quantifying future environmental carrying capacity based on land use/land cover data and ecosystem services valuation: A case study in Makassar City, Indonesia. International Journal of Environmental Studies, 79(4), 686–697. https://doi.org/10.1080/00207233.2021.1941674

Halefom, A., He, Y., Nemoto, T., Feng, L., Li, R., Raghavan, V., Jing, G., Song, X., & Duan, Z. (2024). The impact of urbanization-induced land use change on land surface temperature. Remote Sensing, 16(23), 4578. https://doi.org/10.3390/rs16234502

Hersperger, A. M., Oliveira, E., Pagliarin, S., Palka, G., Verburg, P., Bolliger, J., & Grădinaru, S. (2018). Urban land-use change: The role of strategic spatial planning. Global Environmental Change, 51, 32–42. https://doi.org/10.1016/j.gloenvcha.2018.05.001

Inageoportal. (2024). Portal Data Geospasial BNPB. Badan Nasional Penanggulangan Bencana. https://inageoportal.bnpb.go.id

Islam, A., Pattnaik, N., Moula, M. M., Rötzer, T., Pauleit, S., & Rahman, M. A. (2024). Impact of urban green spaces on air quality: A study of PM10 reduction across diverse climates. Science of the Total Environment, 955, 176770. https://doi.org/10.1016/j.scitotenv.2024.176770

Li, Y., Zhang, J., Sailor, D. J., & Ban-Weiss, G. A. (2019). Effects of urbanization on regional meteorology and air quality in Southern California. Atmospheric Chemistry and Physics, 19(7), 4439–4457. https://doi.org/10.5194/acp-19-4439-2019

Loveland, T. R. (2012). History of land cover mapping (2nd ed.; C. P. Giri, Ed.). CRC Press.

Lu, L., Qureshi, S., Li, Q., Chen, F., & Shu, L. (2022). Monitoring and projecting sustainable transitions in urban land use using remote sensing and scenario-based modeling in a coastal megacity. Ocean and Coastal Management, 224, 106201. https://doi.org/10.1016/j.ocecoaman.2022.106201

Lunetta, R. S., Knight, J. F., Ediriwickrema, J., Lyon, J. G., & Worthy, L. D. (2006). Land-cover change detection using multi-temporal MODIS NDVI data. Remote Sensing of Environment, 105(2), 142–154. https://doi.org/10.1016/j.rse.2006.06.018

Masek, J. G., Honzak, M., Goward, S. N., Liu, P., & Pak, E. (2001). Landsat-7 ETM+ as an observatory for land cover initial radiometric and geometric comparisons with Landsat-5 Thematic Mapper. Remote Sensing of Environment, 78(1–2), 118–130. https://doi.org/10.1016/S0034-4257(01)00254-1

Negesse, M. D., Hishe, S., & Getahun, K. (2024). LULC dynamics and the effects of urban green spaces in cooling and mitigating micro-climate change and urban heat island effects: A case study in Addis Ababa City, Ethiopia. Journal of Water and Climate Change, 15(7), 3033–3055. https://doi.org/10.2166/wcc.2024.662

Radeloff, V. C., Roy, D. P., Wulder, M. A., Anderson, M., Cook, B., Crawford, C. J., Friedl, M., Gao, F., Gorelick, N., Hansen, M., Healey, S., Hostert, P., Hulley, G., Huntington, J. L., Johnson, D. M., Neigh, C., Lyapustin, A., Lymburner, L., Pahlevan, N., … Zhu, Z. (2022). Need and vision for global medium-resolution Landsat and Sentinel-2 data products. Remote Sensing of Environment, 280, 113918. https://doi.org/10.1016/j.rse.2022.113918

Roy, D. P., Wulder, M. A., Loveland, T. R., Allen, R. G., Anderson, M. C., Helder, D., Irons, J. R., Johnson, D. M., Kennedy, R., Scambos, T. A., Schaaf, C. B., Schott, J. R., Sheng, Y., Vermote, E. F., Belward, A. S., Bindschadler, R., Cohen, W. B., Gao, F., … Zhu, Z. (2014). Landsat-8: Science and product vision for terrestrial global change research. Remote Sensing of Environment, 145, 154–172. https://doi.org/10.1016/j.rse.2014.02.001

Shen, Y., Zhang, X., & Yang, Z. (2022). Mapping corn and soybean phenometrics at field scales over the United States Corn Belt by fusing time series of Landsat 8 and Sentinel-2 data with VIIRS data. ISPRS Journal of Photogrammetry and Remote Sensing, 186, 55–69.

https://doi.org/10.1016/j.isprsjprs.2022.01.023

Shen, Y., Zhang, X., Yang, Z., Ye, Y., Wang, J., Gao, S., Liu, Y., Wang, W., Tran, K. H., & Ju, J. (2023). Developing an operational algorithm for near-real-time monitoring of crop progress at field scales by fusing harmonized Landsat and Sentinel-2 time series with geostationary satellite observations. Remote Sensing of Environment, 296, 113729. https://doi.org/10.1016/j.rse.2023.113729

Shrestha, S., Cui, S., Xu, L., Wang, L., Manandhar, B., & Ding, S. (2021). Impact of land use change due to urbanization on surface runoff using GIS-based SCS-CN method: A case study of Xiamen City, China. Land, 10(8), 807. https://doi.org/10.3390/land10080807

Suarmawati. (2023). Development of Investment Promotion Strategy for BauBau City (Vol. 1, Issue 1). BauBau City Investment and One-Stop Integrated Services Office. https://dpmptsp.baubaukota.go.id/upload/publication/publication-20240517171001.pdf

Tran, K. H., Zhang, X., Ketchpaw, A. R., Wang, J., Ye, Y., & Shen, Y. (2022). A novel algorithm for the generation of gap-free time series by fusing harmonized Landsat 8 and Sentinel-2 observations with PhenoCam time series for detecting land surface phenology. Remote Sensing of Environment, 282, 113275. https://doi.org/10.1016/j.rse.2022.113275

U.S. Geological Survey. (2019). Landsat 8 (L8) Data Users Handbook (Version 5.0). USGS. https://landsat.usgs.gov/documents/Landsat8DataUsersHandbook.pdf

Wulder, M. A., Roy, D. P., Radeloff, V. C., Loveland, T. R., Anderson, M. C., Johnson, D. M., Healey, S., Zhu, Z., Scambos, T. A., Pahlevan, N., Hansen, M., Gorelick, N., Crawford, C. J., Masek, J. G., Hermosilla, T., White, J. C., Belward, A. S., Schaaf, C., Woodcock, C. E., … Cook, B. D. (2022). Fifty years of Landsat science and impacts. Remote Sensing of Environment, 280, 113195. https://doi.org/10.1016/j.rse.2022.113195

Wu, H., Lin, A., Xing, X., Song, D., & Li, Y. (2021). Identifying core driving factors of urban land use change from global land cover products and POI data using the random forest method. International Journal of Applied Earth Observation and Geoinformation, 103, 102475. https://doi.org/10.1016/j.jag.2021.102475

Wu, J., Lin, L., Li, T., Cheng, Q., Zhang, C., & Shen, H. (2022). Fusing Landsat 8 and Sentinel-2 data for 10-m dense time-series imagery using a degradation-term constrained deep network. International Journal of Applied Earth Observation and Geoinformation, 108, 102738. https://doi.org/10.1016/j.jag.2022.102738

Yin, J., Dong, J., Hamm, N. A. S., Li, Z., Wang, J., Xing, H., & Fu, P. (2021). Integrating remote sensing and geospatial big data for urban land use mapping: A review. International Journal of Applied Earth Observation and Geoinformation, 103, 102514. https://doi.org/10.1016/j.jag.2021.102514